Available online at www.sciencedirect.com
SCIENCE DIRECT
Hearing Research 218 (2006) 5–19
Hearing Research
www.elsevier.com/locate/heares

Research paper

Interaural delay-dependent changes in the binaural difference potential of the human auditory brain stem response

Helmut Riedel *, Birger Kollmeier

Medizinische Physik, Carl von Ossietzky Universität Oldenburg, D-26111 Oldenburg, Germany

Received 8 June 2005; received in revised form 3 March 2006; accepted 30 March 2006
Available online 9 June 2006

Abstract

Binaural difference potentials (BDs) are thought to be generated by neural units in the brain stem responding specifically to binaural stimulation. They are computed by subtracting the sum of monaural responses from the binaural response, BD = B − (L + R). BDs in dependency on the interaural time difference (ITD) have been measured and compared to the Jeffress model in a number of studies with conflicting results. The classical Jeffress model assuming binaural coincidence detector cells innervated by bilateral excitatory cells via two delay lines predicts a BD latency increase of ITD/2. A modification of the model using only a single delay line as found in birds yields a BD latency increase of ITD. The objective of this study is to measure BDs with a high signal-to-noise ratio for a large range of ITDs and to compare the data with the predictions of some models in the literature including that of Jeffress. Chirp evoked BDs were recorded for 17 ITDs in the range from 0 to 2 ms at a level of 40 dB nHL for four channels (A1, A2, PO9, PO10) from 11 normal hearing subjects. For each binaural condition 10,000 epochs were collected while 40,000 epochs were recorded for each of the two monaural conditions. Significant BD components are observed for ITDs up to 2 ms. The peak-to-peak amplitude of the first components of the BD, DP1-DN1, is monotonically decreasing with ITD. This is in contrast with click studies which reported a constant BD-amplitude for ITDs up to 1 ms. The latency of the BD-component DN1 is monotonically, but nonlinearly increasing with ITD. In the current study, DN1 latency is found to increase faster than ITD/2 but slower than ITD incompatible with either variant of the Jeffress model. To describe BD waveforms, the computational model proposed by Ungan et al. [Hearing Research 106, 66–82, 1997] using ipsilateral excitatory and contralateral inhibitory inputs to the binaural cells was implemented with only four parameters and successfully fitted to the BD data. Despite its simplicity the model predicts features which can be physiologically tested: the inhibitory input must arrive slightly before the excitatory input, and the duration of the inhibition must be considerably longer than the standard deviations of excitatory and inhibitory arrival times to the binaural cells. With these characteristics, the model can accurately describe BD amplitude and latency as a function of the ITD.

Keywords: Binaural difference potential; Interaural time difference; Auditory brain stem response; Delay line; Jeffress model; Chirp; Lateralization; Azimuth

1. Introduction

The interaural time difference (ITD) is one of the most important cues used by the auditory system for azimuthal sound localization (Rayleigh, 1907; Stevens and Newman, 1936; Wightman and Kistler, 1992). The first site of binaural interaction in the mammalian auditory system is the superior olivary complex (SOC) where ITD-sensitive neurons reside. Neurons in the medial superior olive (MSO) predominantly receive excitatory inputs from both cochlear nuclei. These EE-cells are sensitive to ITDs of the fine

Abbreviations: ABR, auditory brain stem response; ACT, acoustic cross talk; B, evoked response to binaural stimulation; BD, binaural difference potential; EE, excitatory–excitatory; IC, inferior colliculus; IE, inhibitory–excitatory; ITD, interaural time difference; L, evoked response to monaural left stimulation; LL, lateral lemniscus; LSO, lateral superior olive; MER, middle ear reflex; MNTB, medial nucleus of the trapezoid body; MSO, medial superior olive; nHL, normal hearing level; R, evoked response to monaural right stimulation; SNR, signal-to-noise ratio; SOC, superior olivary complex; SPL, sound pressure level

* Corresponding author.
E-mail address: helmut.riedel@uni-oldenburg.de (H. Riedel).

0378-5955/$ - see front matter © 2006 Elsevier B.V. All rights reserved.
doi:10.1016/j.heares.2006.03.018

structure of a stimulus in the low-frequency range (<1500 Hz) (Goldberg and Brown, 1968; Yin and Chan, 1990). On the other hand, cells in the lateral superior olive (LSO) primarily receive contralateral inhibitory and ipsilateral excitatory inputs. These IE-cells are sensitive to interaural level differences at higher frequencies (>1500 Hz) (Boudreau and Tsuchitani, 1968; Goldberg and Brown, 1969), but also for ITDs of the stimulus envelope (Joris and Yin, 1995; Joris, 1996; Batra et al., 1997a,b; Joris and Yin, 1998). Furthermore, Tsuchitani (1988a) found that LSO neurons are as well sensitive to ITDs of transients, i.e., to interaural time-of-arrival differences of high-frequency stimuli. The subsequent stages of the mammalian brain stem as the lateral lemniscus (LL) and the inferior colliculus (IC) also exhibit strong ITD sensitivity (Kuwada et al., 1987; Yin et al., 1987; McAlpine et al., 1996; Fitzpatrick et al., 2002; Joris et al., 2004).

The electric activity of the human brain stem can be noninvasively studied with auditory brain stem responses (ABRs, e.g., Jewett et al., 1970; Picton et al., 1974). Specific binaural processing is believed to be reflected by binaural difference potentials (BDs). They are computed as the difference between the binaurally and the sum of monaurally evoked potentials, symbolically $BD = B - (L + R)$ (e.g., Dobie and Norton, 1980; Ito et al., 1988; Jiang, 1996; Riedel and Kollmeier, 2002a). With independent left and right auditory pathways one would obtain $BD = 0$. The amplitude of the binaurally evoked potential is roughly 20% smaller than the sum of the monaurally evoked potentials, i.e., $B < L + R$ (Levine, 1981; McPherson and Starr, 1993; Riedel and Kollmeier, 2002b), resulting in the major negative BD peak named DN1 at or shortly after wave V of the binaural ABR. In studies using the reversed sign convention to compute the BD, the major peak is positive and labeled β (e.g., Levine, 1981; Furst et al., 2004).

The dependence of binaural difference potentials on the ITD has been analyzed in guinea pig (Dobie and Berlin, 1979; Goksoy et al., 2005), cat (Sontheimer et al., 1985; Ungan et al., 1997, 2002) and humans (Wrege and Starr, 1981; Gerull and Mrowinski, 1984; Kelly-Ballweber and Dobie, 1984; Furst et al., 1985, 1990; Jones and Van der Poel, 1990; McPherson and Starr, 1995; Polyakov and Pratt, 1996; Pratt et al., 1997; Brantberg et al., 1999; Riedel and Kollmeier, 2002a; Delb, 2003; Riedel and Kollmeier, 2003; Furst et al., 2004). The results of these studies are partially conflicting and were often interpreted against the background of the model by Jeffress (1948), the prevailing paradigm for azimuthal sound localization for now more than half a century. This model generates a place code for the ITD using an array of coincidence detector cells innervated by excitatory inputs through bilateral delay lines. Postulations regarding the amplitude and the latency of the BD can be derived from the Jeffress model. If BDs would truly reflect the output of Jeffress-like coincidence detector cells, as, e.g., postulated by Jones and Van der Poel (1990) and Furst et al. (2004), a representation of ITDs beyond the physiological range (about ±0.8 ms in humans) would be useless and the BD should vanish at those ITDs. Furst et al. (1985) reported a nearly constant β-amplitude for ITDs up to 0.8 ms, and the BD became undetectable for ITDs > 1 ms. These data support the Jeffress model, and the BD was interpreted a physiological correlate of binaural fusion. Only a few studies tested ITDs beyond the physiological range. Wrege and Starr (1981) found significant BDs for ITDs up to 2 ms, while McPherson and Starr (1995) reported a gradually decreasing BD-amplitude up to an ITD of 1.6 ms. In cat with a physiological ITD-range of roughly ±0.4 ms, Ungan et al. (1997) obtained significant BDs up to ITDs of 1.5 ms.

Regarding the BD latency, the Jeffress model predicts a latency increase (compared to the response to a stimulus with ITD = 0 ms) with half the ITD of the stimulus (Jones and Van der Poel, 1990; Ungan et al., 1997). A modification of the Jeffress model using only a single delay line instead of two as suggested by the projection from the avian nucleus magnocellularis to the nucleus laminaris (Young and Rubel, 1983; Overholt et al., 1992) yields a latency increase of just the ITD of the stimulus (Ungan et al., 1997). The latency increase in human BD studies was reported to be close to the ITD (Wrege and Starr, 1981), close to ITD/2 (Jones and Van der Poel, 1990; Walger et al., 2003) and at intermediate values between ITD/2 and ITD (e.g., Furst et al., 1990; Brantberg et al., 1999; Delb, 2003). In a cat study Ungan et al. (1997) found a nonlinear latency increase between ITD/2 and ITD. They were able to model the amplitude decrease and the latency increase of the BD for a wide range of ITDs with a population model assuming IE-interaction.

With values around 0.2 μV BD amplitudes of humans are comparatively small, and the above-mentioned contradicting results of human studies may in a great measure be attributed to the low signal-to-noise ratio (SNR) of the BD and to insufficient control of the residual noise. Therefore, the objectives of the present study are to measure the ITD-dependence of the BD with high quality and fine ITD resolution for a wide span of ITDs in and outside the physiological range, to investigate if this dependence can be explained by the LSO model proposed earlier (Ungan et al., 1997), and to compare the results to literature data and models of binaural interaction.

2. Methods

2.1. Subjects

Eleven adults, seven males and four females, ranging in age from 23 to 34 years, participated in this study. Subjects were either paid or volunteers from the staff of the Medical Physics Group at the University of Oldenburg. They were classified as normal hearing by routine audiometry and had no history of audiological or neurological problems.

2.2. Stimulation

A chirp signal (Dau et al., 2000) with flat spectrum and nominal edge frequencies of 100 and 14,000 Hz was generated digitally, downloaded to a DSP32C card in the host computer, and DA converted at a sampling rate of 50 kHz. It had a duration of 10.38 ms. The stimuli were amplified by a digitally controlled audiometric amplifier and passed to the subjects via ER-2 (Etymotic Research) insert earphones. In Fig. 1 acoustic waveforms and spectra as measured with a fast Fourier transform (FFT) analyzer (Stanford Research SR780) are shown. A previous study (Riedel and Kollmeier, 2002b) revealed that flat spectrum chirps evoke larger BDs than clicks because of the compensation of basilar membrane dispersion. In contrast to clicks BD amplitudes already saturated at 40 dB nHL. Therefore, the chirps were presented to the subjects at a level of 40 dB nHL corresponding to 82 dB peak equivalent SPL.[1] The time between two subsequent stimulus onsets was chosen to vary randomly and equally distributed between 67 and 77 ms yielding an average stimulation rate of approximately 13.9 Hz.

Besides the two monaural conditions 17 binaural stimuli comprising ITDs from 0 to 1.5 ms in steps of 0.1 ms and additionally 2 ms were employed. The chirp presented to the left ear was delayed by the ITD resulting in a lateralization to the right side. Latency is measured with respect to the leading stimulus, i.e., time zero is at the onset of the right chirp.

In some studies contralateral masking during monaural stimulation has been used to avoid acoustic crosstalk (ACT) (Jones and Van der Poel, 1990; McPherson and Starr, 1995; Brantberg et al., 1999). Ito et al. (1988) proposed randomized stimulation to rule out possible influences of the middle ear reflex (MER). They emphasized a second advantage of randomized stimulation, namely that since all responses are recorded quasi-simultaneously, effects of any slow variation in noise level are reduced so that all averages have the same SNR. In the present study, possible influences of ACT and MER can be ruled out due to the relatively low presentation level of 40 dB nHL. Following Levine (1981) and Ito et al. (1988), left, right and binaural stimuli were presented randomly without contralateral masking.

The stimulation sequence of one run consisted of 12,500 stimuli and was built by concatenating 500 subsequences. The 25 entries of each subsequence were a random permutation of the 17 binaural conditions and four instances of both monaural conditions. One run lasting 15 min therefore consisted of 2000 monaural left, 2000 monaural right, and 500 stimuli for each of the 17 ITD values. A session consisting of 10 runs lasted 2.5 h without preparation and pauses. Two sessions yielding a total of 20 runs were conducted at two different days. A total of 250,000 stimuli was presented to every subject: 40,000 monaural left chirps, 40,000 monaural right chirps, and 10,000 binaural stimuli for each of the 17 ITD conditions.

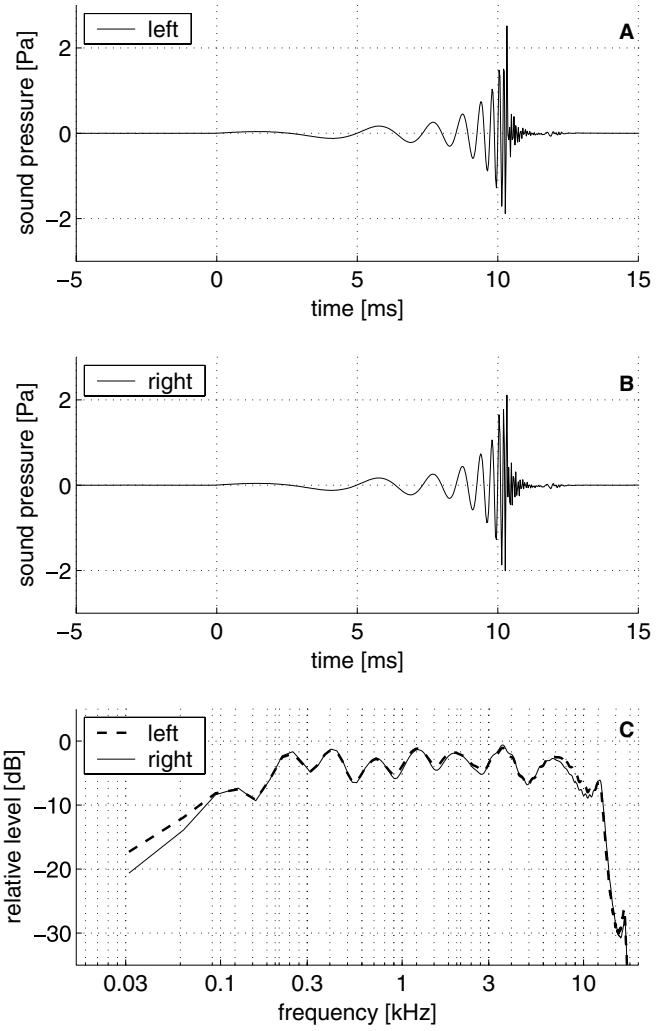

Fig. 1. (A) Acoustic waveform of the left chirp. (B) Acoustic waveform of the right chirp. (C) Acoustic spectra of the left (thick, dashed) and right (thin, solid) stimulus using a frequency resolution of 31.25 Hz. Measurements were performed at a level of 60 dB nHL corresponding to 102 dB peSPL.

2.3. Recordings

For the ABR recordings Ag/AgCl-electrodes were used. The 4 active channels were placed at the left (A1) and right (A2) mastoid and the parieto-occipital positions PO9 and PO10 according to the extended 10–20-system (Jasper, 1957; Sharbrough et al., 1991). The common reference electrode was placed at the vertex (Cz), the ground electrode at the forehead (Fpz). Electrode impedances were measured at a test signal frequency of 30 Hz and brought well below 5 kΩ, common values were 2–3 kΩ. Since DC recordings

[1] A sinusoid of frequency 1 kHz with the same peak-to-peak-amplitude as the chirp showed 82 dB sound pressure level in a Brüel & Kjær (B&K) amplifier type 2610. The calibration was performed using a half inch microphone (B&K 4157) with an artificial ear (1.29 cm^3) and a preamplifier (B&K 2669).

were performed, the criteria for a good contact between electrodes and skin were both a low impedance and a vanishing voltage drift seen in the raw EEG signal.

During the ABR recordings, subjects lay in a sound insulated and electrically shielded room. They were instructed to relax and lie as comfortably as possible. ABR were recorded with a DC-coupled differential amplifier (Synamps 5803). Inside the shielded room the EEG was preamplified by a factor 150, further amplified by the main amplifier by a factor 33 resulting in a total amplification of 74 dB. The voltage resolution was approximately 16.8 nV/bit. The raw continuous EEG was filtered by an analog antialiasing-lowpass filter with an edge frequency of 2 kHz, digitized with 10 kHz samplingrate and 16 bit resolution, and stored to hard disk. The time instances of stimulus begin and the stimulus conditions were also recorded in the raw EEG file by means of a digital trigger port. The clipping level of the DA-converters was $\pm 550\,\mu V$, the artifact level was set to $\pm 500\,\mu V$, since filtering, artifact analysis and averaging was done offline.

2.4. Data analysis

Epochs of 55 ms duration including a prestimulus interval of 15 ms belonging to the same stimulus conditions were cut out of the continuous EEG and filtered with a linear phase FIR bandpass filter with 200 taps and the edge frequencies 100 and 1500 Hz (Granzow et al., 2001). An iterated weighted average of the filtered sweeps was computed for all subjects and stimulus conditions. The residual noise of the averages was calculated as the time-averaged standard error of the single sweeps σ (Riedel et al., 2001).

For all stimulus conditions, the binaural difference potential was computed for all channels and sample by sample. For the stimuli with non-zero ITD the monaural left response was digitally delayed by the ITD before computing the binaural difference potential: $BD_{ITD}(t) = B(t) - (L(t - ITD) + R(t))$. The residual noise, i.e., the standard error of the BD, was estimated as the square root of the summed variances of the three measurements assuming their mutual statistical independence: $\sigma_{BD} = (\sigma_B^2 + \sigma_L^2 + \sigma_R^2)^{1/2}$.

By presenting the monaural conditions more often than the binaural conditions, σ_{BD} can be reduced because the monaural responses, and therefore σ_L and σ_R, enter the computation of the BD for all ITDs. For a given measurement time, i.e., total number of sweeps, it is optimal to present both monaural stimuli $\sqrt{b}$ times more frequently than each of the b different binaural stimuli. The proof and an expression for the reduction of σ_{BD}, or equivalently, the improvement in signal-to-noise ratio (SNR), compared to the standard procedure using equal sweep numbers for binaural and monaural stimuli, is given in the appendix. Nevertheless, this procedure using constant sweep numbers does not guarantee equal or high SNRs for the different subjects. In the present study, the reduction of the standard error of the BD achieved by presenting the monaural stimuli four times more often than the binaural conditions amounts to 18.4%. The same reduction would have been obtained in the standard stimulation scheme with equal sweep numbers by prolonging the measurement time by 50%.

The accuracy of amplitude and latency measurements was increased by upsampling the averaged data by a factor of 10, i.e., changing the sampling rate from 10 to 100 kHz. This was accomplished by zero-padding in the spectral domain which in the time domain corresponds to a convolution with a sinc-function. Since the original analog signal was band-limited to frequencies below 2 kHz a near-to-perfect interpolation was possible. Peaks in the interpolated signal were identified by a sign change in its derivative. For baseline-to-peak-measurements peaks with voltages V_{bp} smaller than $3\sigma_{BD}$ (99.7% confidence level for Gaussian measurement errors) were not regarded as significant and hence were discarded. The 3σ-criterion was proposed by Stollman et al. (1996) and found to be superior to a template matching method for the detection of significant BD components. However, the measurement of the residual noise σ, and therefore, the detection of significant BD components, is far more accurate in the present study since it relies on the analysis of single sweeps in contrast to the conventional methods relying on the comparison of two (sub-)averages or the variance in the averaged prestimulus interval (Granzow et al., 2001; Riedel et al., 2001). For peak-to-peak-measurements peaks with voltages V_{pp} greater than $\sqrt{2} \cdot 3\sigma_{BD}$ were accepted. The additional factor of $\sqrt{2}$ is due to the fact that the variances of both peaks in the pair add up. Latency errors were estimated from the amplitude errors and the curvature of the peaks according to Hoth (1986). The first main component of the BD is the negative wave DN1 preceded by a smaller positive wave labeled DP1. The nomenclature introduced by Ito et al. (1988) is adopted here (see their Fig. 1). DN1 corresponds to the β-wave described by Levine (1981). BD latencies of the larger component DN1 were analyzed, amplitudes were measured peak-to-peak from DP1 to DN1.

2.5. Model

A model to explain the dependency of BD latency and amplitude versus ITD was proposed by Ungan et al. (1997) for cat data. This model is adopted and implemented here to describe human BD data. The binaural reduction generally found in BD studies is reflected in the model by binaural cells achieving contralateral inhibitory and ipsilateral excitatory inputs (IE-cells) associated with binaural interaction found in the LSO. The model has only four parameters:

(1) The difference between mean arrival times of the excitatory and the inhibitory input to the binaural cell $t_{e-i} = t_e - t_i$.
(2) The standard deviation of the arrival time of the excitatory input σ_e.

(3) The standard deviation of the arrival time of the inhibitory input σ_i.
(4) The duration of inhibition of the binaural (LSO) cell τ_i.

The inhibition caused by the contralateral input is assumed to be effective for a time interval τ_i. An excitatory input cannot fire the LSO cell if it arrives during the inhibited interval, i.e., if $t_i < t_e < t_i + \tau_i$. The model accounts only for relative quantities: the normalized BD amplitude and the latency increase of the BD relative to ITD = 0 ms. To incorporate the absolute BD amplitude and latency into the model, two additional parameters which can be derived from the diotic response would be required: an absolute amplitude factor a and the arrival time of the excitatory input t_e. The BD amplitudes and latencies of the model are derived from simulated BD waveforms which are computed as follows. Arrival times of the excitatory and inhibitory inputs are assumed to follow normal distributions. The distribution of the excitatory input from left cochlear nucleus (CN) to the left LSO is affected by the ITD:

$$L_e(t, \mathrm{ITD}) = \frac{a}{\sqrt{2\pi}\sigma_e} \exp\left(\frac{-(t - t_e - \mathrm{ITD})^2}{2\sigma_e^2}\right). \quad (1)$$

The distribution of the excitatory input to the right LSO is not delayed by the ITD:

$$R_e(t) = \frac{a}{\sqrt{2\pi}\sigma_e} \exp\left(\frac{-(t - t_e)^2}{2\sigma_e^2}\right). \quad (2)$$

The distribution of the contralateral inhibitory inputs is described by the difference of two cumulative normal distributions, the inhibitory input from the right side to the binaural cell in the left LSO is

$$L_i(t) = \frac{a}{\sqrt{2\pi}\sigma_i} \int_{t-\tau_i}^{t} \exp\left(\frac{-(t' - t_i)^2}{2\sigma_i^2}\right) \mathrm{d}t' \quad (3)$$

The inhibitory input from the left side to the binaural cell in the right LSO is

$$R_i(t, \mathrm{ITD}) = \frac{a}{\sqrt{2\pi}\sigma_i} \int_{t-\tau_i}^{t} \exp\left(\frac{-(t' - t_i - \mathrm{ITD})^2}{2\sigma_i^2}\right) \mathrm{d}t' \quad (4)$$

Fig. 2A and B show the inputs to the binaural cells in the left and right LSO, respectively, for all ITDs applied. The modeled BD is computed for both LSOs separately. The output of the left LSO cell to left (excitatory) input is L_e, zero to right (inhibitory) input and $L_e(1 - L_i)$ to binaural input. To describe that no activation of the binaural cell can occur during inhibitory activation in the time interval from $t_i - \tau_i$ to τ_i, the inhibition is modeled in a multiplicative manner. The contributions of the left (Fig. 2C) and right (Fig. 2D) LSO to the BD are

$$\mathrm{BD_L} = L_e(1 - L_i) - L_e, \quad \mathrm{BD_R} = R_e(1 - R_i) - R_e, \quad (5)$$

respectively. The contribution of the left (contralateral) LSO to the BD is larger than the contribution of the right LSO, especially for large ITDs. Due to the small distance of the generator sites (left and right LSO) compared to the distance to the far field electrodes, the generators can reasonably be approximated by a single central generator. Therefore, the modeled BD is assumed to be simply the sum of the two contributions: $\mathrm{BD} = \mathrm{BD_L} + \mathrm{BD_R}$.

In contrast to the study by Ungan et al. (1997) where the model parameters were derived from physiological data and subsequently adjusted manually, in the present study these parameters are optimized by means of a χ^2-fit of the average BD amplitude and latency data over subjects. We name the measured and modelled BD amplitudes A_k and A'_k after normalization, respectively, with k being the index of the ITD. The normalized measured and modelled BD latencies shall be denoted by t_k and t'_k, respectively. The interindividual standard deviations of the measured BD amplitudes and latencies are denominted by $\sigma_{A,k}$ and $\sigma_{t,k}$, respectively. The simplex algorithm (Nelder and Mead, 1965) was used to minimize the cost function

$$e = \sum_{k=2}^{17} \left(\frac{A_k - A'_k}{\sigma_{A,k}}\right)^2 + \sum_{k=2}^{17} \left(\frac{t_k - t'_k}{\sigma_{t,k}}\right)^2 \quad (6)$$

The sums include only 16 out of the 17 ITDs measured because the normalization eliminated the variance for the data at ITD = 0 ms. The optimal solution found by the algorithm was virtually insensitive to the starting values of the four parameters.

3. Results

3.1. Measured binaural difference potentials

Fig. 3 shows chirp evoked BDs for ITDs between 0 and 2 ms for one subject and a single recording channel. BD latencies are about 10 ms longer than in click studies since they are measured from the onset of chirp. For all ITDs the BD peaks DP1 and DN1 are significant, i.e., the peak-to-peak amplitude $A_{\mathrm{DP1\text{-}DN1}}$ exceeds $\sqrt{2} \cdot 3$ standard errors of the measurement. BD amplitude is decreasing and BD latency is increasing with increasing ITD.

In Fig. 4 the peak-to-peak amplitude $A_{\mathrm{DP1\text{-}DN1}}$ averaged over the four measurement channels is depicted for all 11 subjects with intraindividual standard errors. The mean amplitude averaged over subjects with interindividual standard deviations is shown in the lower right panel. Generally, BD amplitude is decreasing as ITD increases, but in some subjects the maximal BD is found at small ITD values (0.1 or 0.2 ms). There is strong interindividual variation in BD amplitude, for ITD = 0 ms $A_{\mathrm{DP1\text{-}DN1}}$ varies between 0.13 and 0.42 μV. Significant BD components are still observable for ITDs up to 2 ms. The mean BD peak-to-peak amplitude averaged over subjects decreases from 0.240 μV for ITD = 0 ms to 0.169 μV at ITD = 1 ms and to 0.144 μV at ITD = 2 ms. Due to the randomized stimulation the residual noise does virtually not change with ITD, but it varies among subjects between 17 and 46 nV

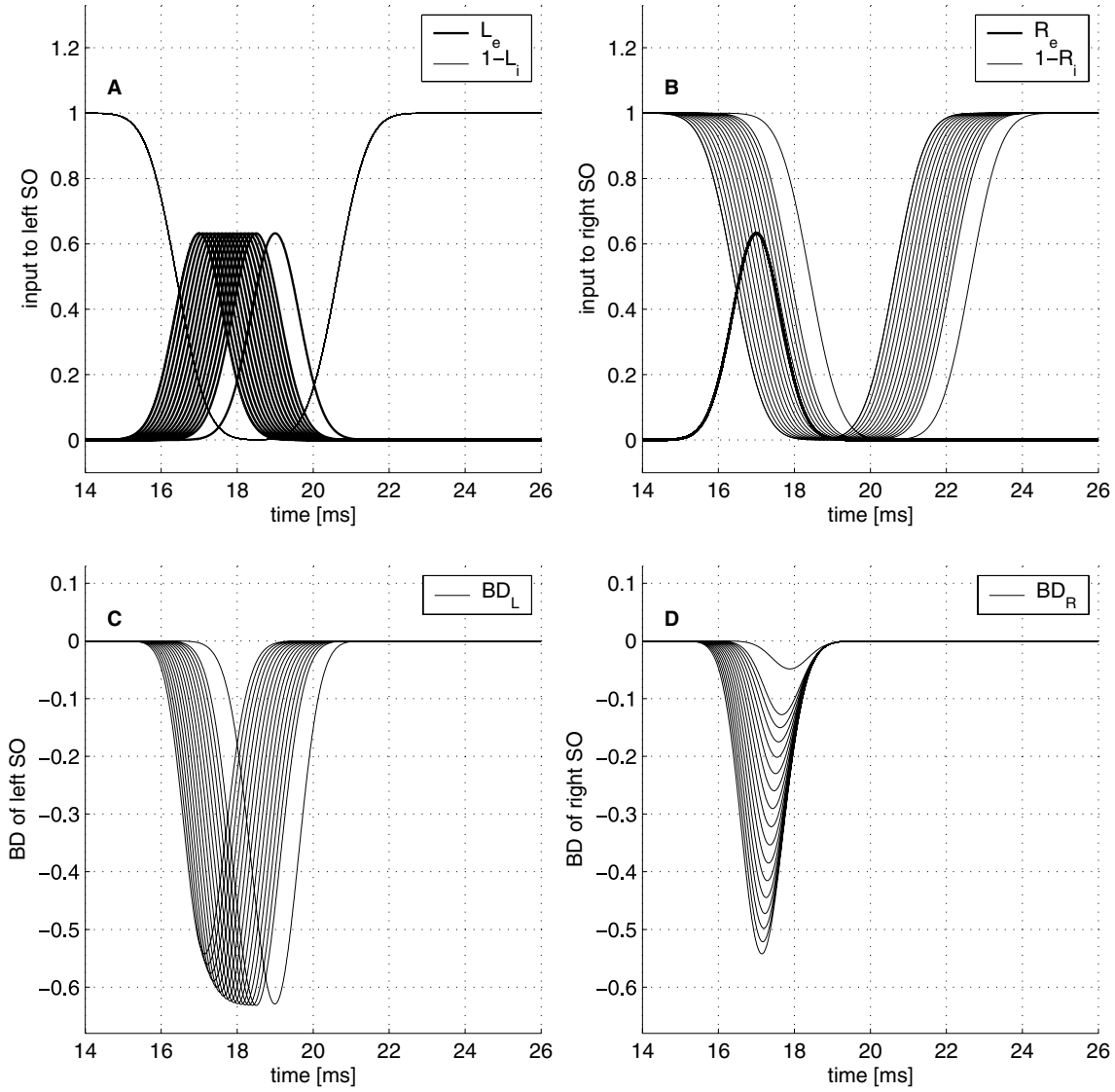

Fig. 2. In every subplot the array of curves corresponds to the ITDs used in the measurements, ranging from 0 ms to 1.5 ms in steps of 0.1 ms. Additionally an ITD of 2 ms was applied. (A) Time courses of the inputs to the left LSO: ipsilateral excitation is delayed by ITD (thick), contralateral inhibition (thin) is not affected by ITD. (B) Time courses of the inputs to the right LSO: ipsilateral excitation (thick) is not affected by ITD, contralateral inhibition (thin) is delayed by ITD. (C) BDs in the left LSO as function of the ITD. (D) BDs in the right LSO as function of the ITD.

(mean 28 nV). The SNR for diotic stimulation ranges between 3.8 and 23.9 (mean 9.3). For the largest ITD of 2 ms, SNR-values are between 3.1 and 11.4 (mean 5.5).

The DN1-latency t_{DN1} averaged over channels is plotted in Fig. 5 for all 11 subjects with intraindividual standard errors. The mean latency averaged over subjects with interindividual standard deviations is shown in the lower right panel. The shortest latency is always found for diotic stimulation, DN1 latency is virtually monotonically increasing with increasing ITD. The slope of the latency function is flatter for smaller ITDs and steeper for larger ITDs.

3.2. Modeled binaural difference potentials

The χ^2-fit of the model parameters to the data revealed a faster contralateral travel time of the inputs to the binaural cell: $t_{e-i} = 0.597$ ms. The standard deviations of the arrival time distributions were virtually identical for excitatory and inhibitory inputs: $\sigma_e = 0.631$ ms, $\sigma_i = 0.629$ ms. The width of the inhibition window was fitted to $\tau_i = 4.23$ ms. The waveforms obtained in this way are depicted in Fig. 6. The model was not designed to describe the small component DP1 preceding DN1, however, it mirrors the main features of the recorded BDs, as shown in Fig. 3. The simulated DN1 amplitude decreases and DN1 latency increases with increasing ITD. To roughly match amplitude and latency of the data in Fig. 3, the amplitude factor a was set to 0.44 and the arrival time of the excitatory input t_e to 16.6 ms.

Fig. 7 gives a comparison of the normalized modeled and measured BD amplitude. Before averaging over subjects the BD amplitude was normalized by dividing by

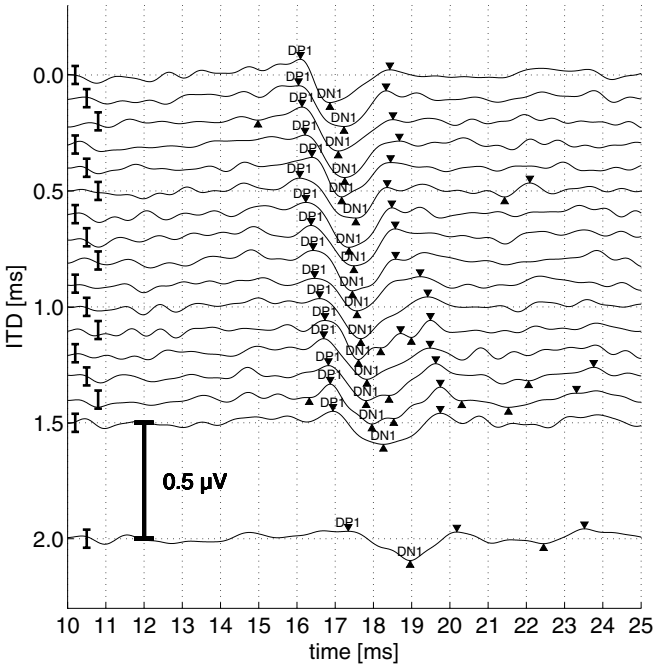

Fig. 3. BDs in dependence on the ITD: data from channel PO10, subject rh. The error bars denote ±3 standard errors of the mean ($\pm 3\sigma$). The triangles indicate peak pairs whose peak-to-peak values exceed $\sqrt{2} \cdot 3\sigma$. The time axis is plotted relative to stimulus onset of the leading chirp presented to the right ear. Significant binaural interaction is found for all ITDs tested. The BD-peaks DP1 and DN1 occur slightly before and after the latency of the binaural wave V, respectively.

the values for ITD = 0 ms since the model predicts amplitude ratios, but no absolute amplitudes. The model seems to underestimate the measured amplitudes for small ITDs in the range up to 0.4 ms. In this range, the data appear to be relatively constant while the model predicts a monotonically decreasing BD amplitude. However, taking into account the standard deviation of the mean data over subjects, the model explains the data very well. The goodness-of-fit is almost one.

In Fig. 8 the modeled and measured normalized DN1 latencies are compared. Since absolute latency is not an issue of the model, DN1 latency was normalized by subtracting the values for ITD = 0 ms before averaging over subjects. For ITDs up to 0.3 ms the latency increase is approximately ITD/2 as in the Jeffress model with a double delay line (lower straight line with the slope ITD/2). However, for larger ITDs the Jeffress model strongly underestimates the measured latency increase. In contrast, the modified Jeffress model using a single delay line (upper straight line with slope ITD) overestimates the growth of the BD latency.

Unlike the two variants of the Jeffress model, the model employed well explains the BD latency increase as function of the ITD. In addition, while the Jeffress model does not yield explicit BD amplitude predictions, the model studied here also correctly describes the BD amplitude as function of the ITD.

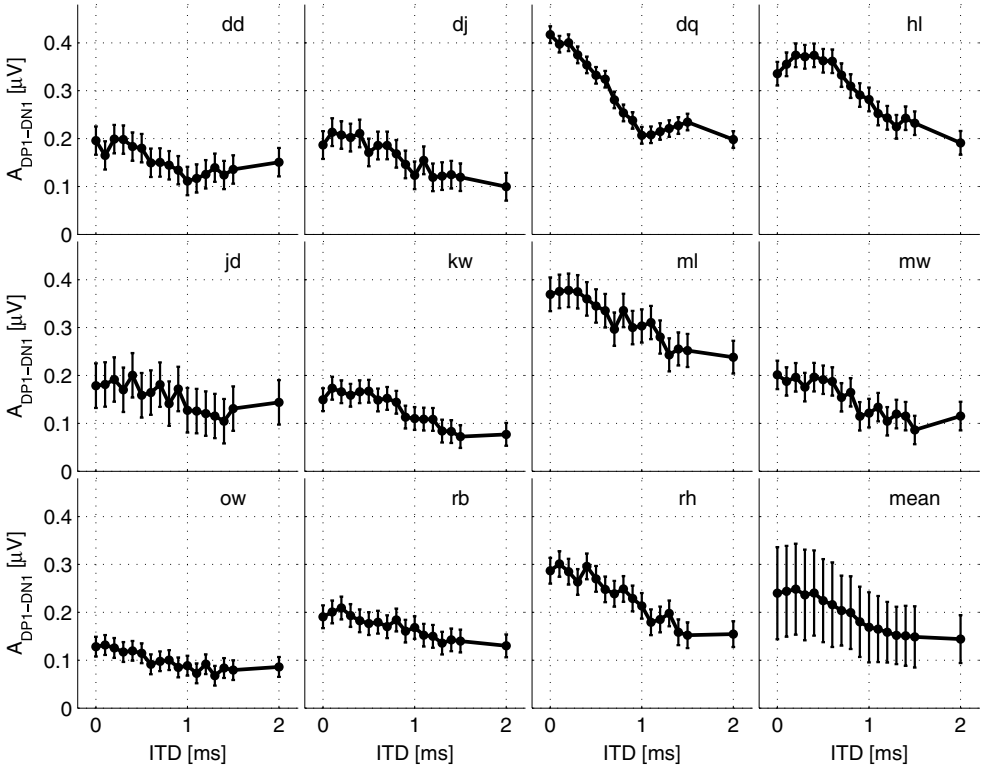

Fig. 4. Mean amplitude of BD-wave DP1-DN1 averaged over channels as function of the ITD. The first 11 panels show single subject data, the error bars indicate intraindividual standard errors ($\pm\sqrt{2} \cdot \sigma$). The last lower right panel depicts the mean over subjects, the error bars denote ±1 standard deviation.

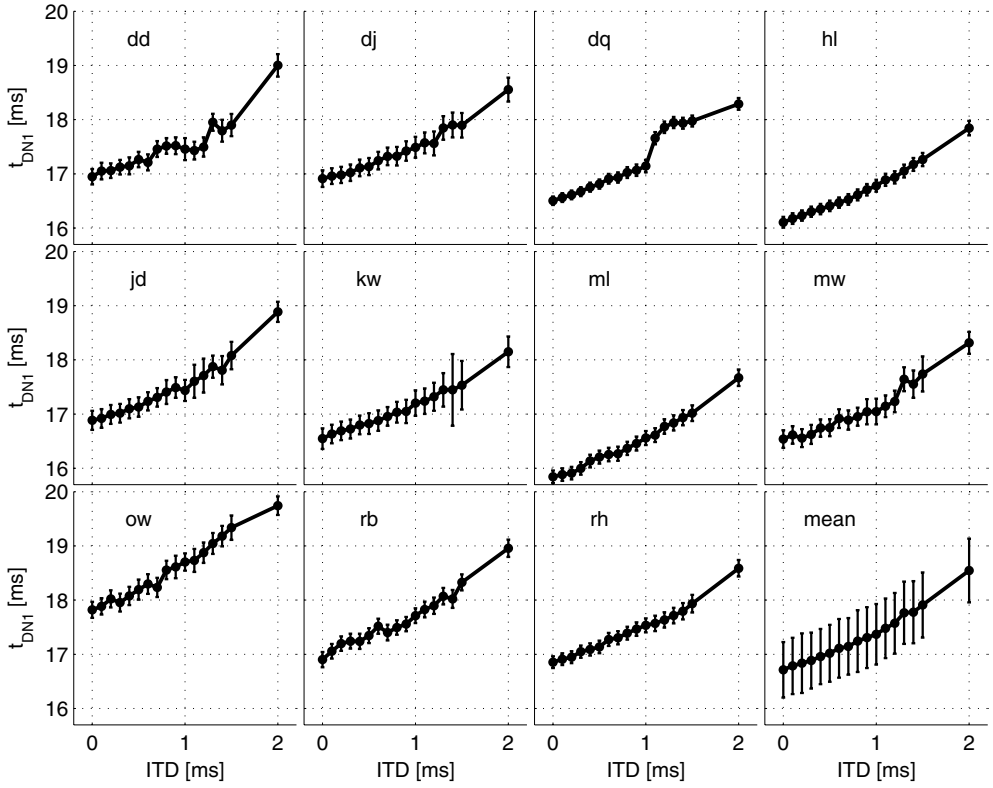

Fig. 5. Mean latency of BD-wave DN1 averaged over channels as function of the ITD. The first 11 panels show single subject data, the error bars indicate $\pm 3\sigma$. The last lower right panel depicts the mean over subjects, the error bars denote ± 1 standard deviation. Latencies are measured from the onset of the leading stimulus.

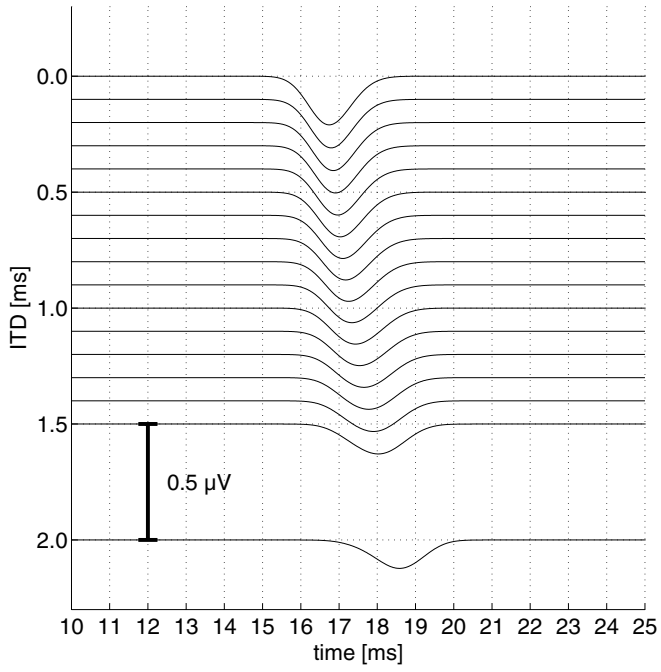

Fig. 6. DN1 waves simulated with the set of model parameters that provide the best fit to the averaged human data in Figs. 4 and 5. As in the experimental data (Fig. 3) DN1 amplitude decreases and DN1 latency increases with increasing ITD.

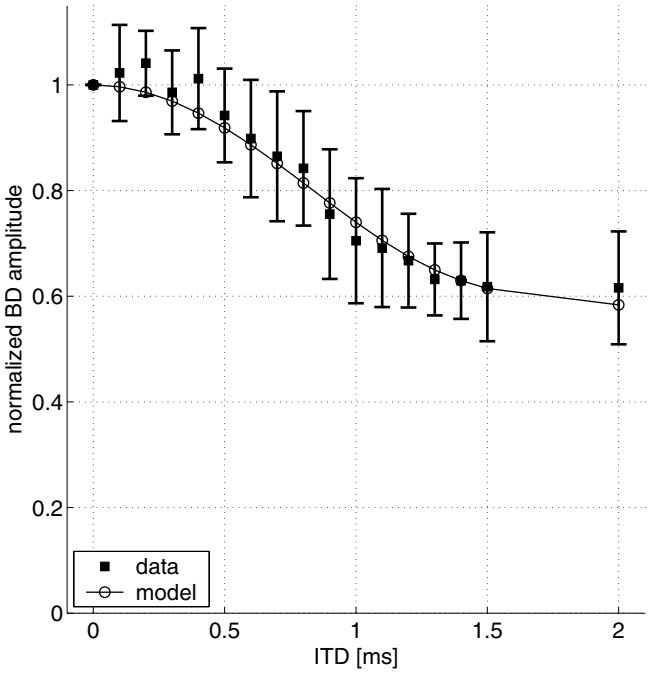

Fig. 7. Comparison of measured and modeled BD amplitudes: the squares denote normalized BD amplitudes $A_{\mathrm{DP1\text{-}DN1}}/A_{\mathrm{DP1\text{-}DN1}}(\mathrm{ITD}=0)$, error bars designate ± 1 standard deviation. The open circles connected by lines indicate the modeled BD amplitudes.

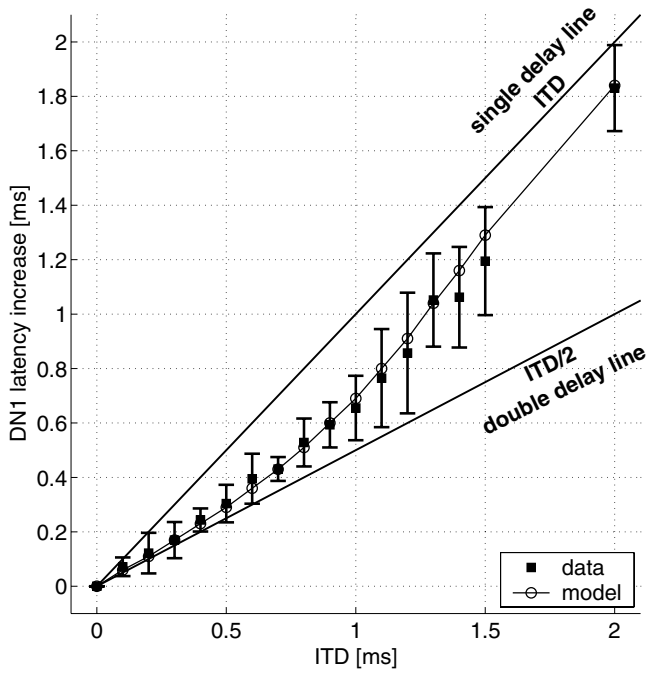

Fig. 8. Comparison of measured and modeled BD latencies: the squares denote normalized DN1 latencies $t_{DN1} - t_{DN1}(ITD = 0)$, error bars designate ±1 standard deviation. The circles connected by lines indicate the modeled BD latencies. The lower line with the slope ITD/2 shows the latency increase predicted by the original Jeffress model using two delay lines. The upper line with unit slope depicts the latency increase of a modified model with only one delay line.

4. Discussion

Binaural difference potentials were measured in dependence on the ITD using a high temporal resolution of 0.1 ms in the range from 0 to 1.5 ms, i.e., about twice the human physiological range. Large sweep numbers, an improved stimulation paradigm (40,000 sweeps for the monaural stimuli, 10,000 sweeps for the binaural stimuli) and the use of the chirp stimulus ensured the high quality (SNR) of the data. Therefore, systematic dependencies of BD amplitude and latency on the ITD could be discovered even for individual subjects. Three advantages of the chirp stimulus due to an improved synchonisation of basilar membrane activity (Dau et al., 2000) have to be emphasized: First, the BD amplitude is larger for chirps than for clicks. Second, the growth function of the BD amplitude already saturates at about 40 dB nHL (Riedel and Kollmeier, 2002b). At such a low presentation level as used in the present study, contributions from ACT and MER (Levine, 1981) are implausible underlining the notion that binaural difference potentials truly reflect specific binaural processes in the brain stem. Last but not least, the relatively low presentation level was rather comfortable for the subjects, an advantage which can barely be overestimated in an experiment with many hours of measurement time for every subject.

4.1. BD amplitude

The comparison of BD amplitudes between different studies is complicated by the fact that in some studies the baseline-to-peak amplitude DN1 (or β) was used while others measured the peak-to-peak amplitude DP1-DN1. In the present study, we followed the latter approach. However, if we measured BD amplitude from baseline to peak, our principal results would be virtually the same since DN1 amplitudes are roughly two thirds of the DP1-DN1 amplitude independent of ITD.

Literature data on human BD amplitude in the dependence on the ITD are conflicting. Polyakov and Pratt (1996), Brantberg et al. (1999) and Delb (2003) found an approximately constant click evoked BD amplitude up to an ITD of 1 ms, but did not measure BDs for longer ITDs. Brantberg et al. (1999) provide BD amplitudes in their Table 1 for 12 subjects. A plot of these data reveals highly irregular dependencies of DN1 amplitude on ITD for the single subjects. DN1 amplitudes decrease, increase or are strongly nonmonotonic functions of the ITD for different subjects. Apparently, averaging 4096 single responses was not sufficient to obtain consistent functions for the single subjects casting their main conclusion into doubt that BD amplitude does not vary with ITD.

Furst et al. (1985) reported a nearly constant DN1 amplitude up to an ITD of 0.8 ms, but for ITDs larger than 1 ms, BD was undetectable. However, considering that their BD amplitude was plotted on a dB scale (see their Fig. 3a), the constancy of the BD amplitude is less pronounced. Because BDs were found in the human physiological range (about ±0.8 ms), but not outside, they were interpreted as physiological correlate of binaural fusion. Given the restriction of binaural interaction to naturally occuring ITDs, these data implicitly support the Jeffress model, because coincidence detection is not needed outside the physiological range and has hence not developed.

On the other hand, McPherson and Starr (1995) found monotonically decreasing BDs when the ITD was increased from zero to 1.6 ms. However, as pointed out by Brantberg et al. (1999), McPherson and Starr (1995) reported comparably large BD components (0.92 μV at ITD = 0 ms) and longer BD latencies than in the other studies invalidating the comparison. For ITDs of ±0.4 ms using clicks at 60 dB nHL, Riedel and Kollmeier (2002a) measured a small, but significant amplitude decrease to 89% of the value for diotic stimulation. In close agreement to the present study, Jones and Van der Poel (1990) found virtually no DN1 (their 'P1') amplitude reduction at an ITD of 0.4 ms compared to diotic stimulation, but reported a reduction to 78% at an ITD of 0.8 ms. Walger et al. (2003) measured the peak-to-peak amplitude of the click-evoked BD for the ITDs 0, 0.3 and 0.6 ms and found a slightly sharper decrease compared to the present study: on average, the amplitude difference DP1-DN1 decreased to 74% at 0.3 ms and to 57% at 0.6 ms ITD.

Except for the early work by Wrege and Starr (1981) with only two subjects and the study by McPherson and Starr (1995) human BD studies did either not consider ITDs larger than 1 ms or did not find significant components at these longer ITDs.

In the present study, the peak-to-peak amplitude DP1-DN1 is approximately constant up to an ITD of only 0.4 ms. In contrast to the click studies from Furst et al. (1985) and Brantberg et al. (1999), normalized BD amplitude drops to about 70% for an ITD of 1 ms and to roughly 60% for an ITD of 2 ms which is far outside the human physiological range (Fig. 7). Unlike the study by Furst et al. (1985), no sharp decrease near the border of the physiological range (about ±0.8 ms in humans) was observed.

On the one hand, the monotonic decrease of the chirp evoked BD amplitude enfeebles the assertion that the BD can be regarded as a electrophysiological correlate of binaural fusion (Furst et al., 1985, 1990). On the other hand, significant BDs for ITDs as long as 2 ms can be used to argue against the Jeffress model: if the BD would indicate activity of coincidence detectors connected to delay lines (Jones and Van der Poel, 1990; Furst et al., 2004), it would be incomprehensible why delays longer than twice the physiological range should be represented in the binaural system.

Ungan et al. (1997) measured BD amplitude as a function of the ITD in cat using click stimuli. In accordance with the present study they reported a monotonic decrease of DN1 amplitude with increasing ITD, and at the border of the cat's physiological range (about 0.4 ms) no transition was observed.

4.2. BD latency

As pointed out by Ungan et al. (1997), the latency increase of the BD should be a linear function of the ITD if the Jeffress model holds. The latency increase of the original model using two delay lines is ITD/2. If only a single delay line as found in the avian system (Young and Rubel, 1983; Carr and Konishi, 1990) is assumed, the latency increase is simply given by the ITD. Therefore, the analysis of the relative latency of the major BD component DN1 (or β) provides an indirect test of the Jeffress model. Jones and Van der Poel (1990) reported a latency increase of ITD/2 up to ITDs of 0.5 ms and interpreted this finding as corroboration of the original double delay line model by Jeffress. However, at ITDs larger than 0.5 ms, relative DN1 latency grew stronger than ITD/2, at an ITD of 1 ms the latency increase was about 0.71 ms, see their Fig. 2. Furst et al. (1990) reported a roughly linear β-latency increase up to ITDs of 0.8 ms with a slope of 0.6. In the studies by Polyakov and Pratt (1996) and Pratt et al. (1997) ITDs of 0.2, 0.4 and 1 ms were used to derive binaural difference potentials, but latency values were not listed. From Fig. 6 in Pratt et al. (1997) it can be inferred that at an ITD of 1 ms, DN1 (their 'P1') latency increase was approximately 0.7 ms. Brantberg et al. (1999) plotted absolute mean DN1 latencies in their Fig. 4 showing a systematic increase with ITD. The latency increase could be inferred from their Table 1. Like the amplitudes, the latencies varied enormously over subjects: for ITD = 0.39 ms, e.g., the increase was 0.76 ms for subject 11, but was negative (−0.05 ms) for subject 6. On average over subjects, the latency increase is 0.54*ITD for ITD = 0.19 ms and between 0.7*ITD and 0.75*ITD for ITDs ranging from 0.39 to 0.99 ms. Riedel and Kollmeier (2002a) found a latency increase of 0.21 ms for an ITD of ±0.4 ms. Walger et al. (2003) reported a latency increase of about ITD/2 for the ITDs 0.3 and 0.6 ms while Delb (2003) measured an approximately linear DN1 latency increase of 0.7*ITD and mentioned the inconsistency of this finding with the Jeffress model. Furst et al. (2004) a priori assumed a linear DN1 latency increase and reported slopes of 0.5 for adults and 0.56 for newborns. However, with increasing ITD the detectability of DN1 dropped dramatically in infants, introducing a bias towards the DN1 latencies for smaller ITDs. In the case of the adults, no statement on DN1 detectability as function of the ITD was made.

The data of the present study reveal a latency increase of ITD/2 only up to ITDs of 0.3 ms. For larger ITDs, DN1 latency increase is between ITD/2 and ITD. Due to the high number of single sweeps measured, the systematic BD latency increase is visible for all single subjects, see Fig. 5. The best linear fit to the mean data has a slope of 0.7. This is in accordance with the data from Pratt et al. (1997), Brantberg et al. (1999) and Delb (2003). However, the fine ITD resolution of the present study reveals that a linear fit inadequately describes the nonlinear latency dependence on the ITD. A quadratic fit ($0.50*\mathrm{ITD} + 0.20*\mathrm{ITD}^2$) better describes the data, but is of little explanatory value. As for the amplitude data, our latency data are in principle in good accordance with the cat data by Ungan et al. (1997). Therefore, the model developed by Ungan et al. (1997) for the cat was adopted and implemented to describe human BD data.

4.3. BD model and generation

The model adopted from Ungan et al. (1997) describes the nonlinear dependence of BD amplitude and latency on the ITD with only four parameters very well. The model parameters for humans are all larger than the parameters for cat. Ungan et al. (1997) found a larger standard deviation for the excitatory arrival time than for the arrival time of the inhibition ($\sigma_e = 0.4$ ms, $\sigma_i = 0.12$ ms) while for the human model both values are nearly identical (0.63 ms). In a recent article, Goksoy et al. (2005) applied the same model to guinea pig data and found comparable standard deviations of the arrival times ($\sigma_e = 0.17$ ms, $\sigma_i = 0.23$ ms). Both, human and cat model, yield a faster arrival of the contralateral inhibitory input compared to the ipsilateral excitatory input. This advance of the inhibition was 0.1 ms in cat and nearly 0.6 ms in the human model and is a critical feature of the model. With equal

excitatory and inhibitory arrival times or a lag of the inhibition in the model, the decrease of the BD amplitude with the ITD would be too weak compared to the data. At the first glance, an earlier arrival of the contralateral inhibition seems surprising given the longer pathway and the additional synapse in the medial nucleus of the trapezoid body (MNTB). Physiological data on this topic are conflicting. In cat Joris et al. (1998) reported a lag of the contralateral arrival in the LSO of 0.2 ms, while Tsuchitani (1988) in her cat LSO study pointed out that 'both the fast transmission path from the CN to the MNTB and the location of the MNTB terminals on the LSO body ensure that the contralateral input can influence the spike generator of an LSO neuron before ipsilateral input'. The length of the inhibition τ_i was 1.8 ms in the cat study by Ungan et al. (1997) and 4.2 ms in the present study. An analysis of the accuracy of the model parameters shows that only a lower bound for τ_i of about 3.3 ms can be defined, but that τ_i can be prolonged to arbitrarily long values without hampering the goodness of fit very much. To estimate an upper bound of τ_i, one would have to measure BDs using stimuli with very long ITDs. Thus, the model predicts a long-lasting inhibition which can be tested physiologically.

The possible BD generators were discussed controversially in literature. Caird and Klinke (1983) reported smaller time-intensity-trading ratios for MSO than for LSO cells. Given the relatively small time-intensity-trading ratios needed to obtain a maximal BD amplitude, Sontheimer et al. (1985) suggested the MSO as site of BD generation. In her cat study, Melcher (1996) supported this hypothesis by lesion experiments and excluded the LSO as possible BD generator. Levine and Davis (1991) measured BDs in the presence of a high pass masker and concluded that the frequency region above 4 kHz largely accounts for the BD. They suggested that the subpopulation of high frequency units in the MSO might be the possible BD generator excluding the LSO because it is much less prominent in man compared to the MSO. However, given the larger percentage of high-frequency cells in the LSO, the results of the study by Levine and Davis (1991) could also be interpreted as a hint that the LSO is the main BD generator.

On the other hand, a large body of evidence suggests the LSO with its predominant IE-interaction as main BD generator. BD studies report a binaural reduction in all species, i.e., the binaurally evoked potential is always smaller than the summed monaural response ($B < L + R$). Therefore it is unlikely that EE-interaction as found in the MSO (Goldberg and Brown, 1968; Yin and Chan, 1990) is the main BD source. In their guinea pig study Wada and Starr (1989) concluded from the observed binaural reduction that EE-interaction was not in evidence. McPherson and Starr (1993) stated that the form of binaural interaction is a relative decrease and therefore suggest that 'inhibition may be the major mechanism utilized in binaural processes'.

Nevertheless, a possible contribution of EE-cells in the MSO to the BD could be generated by saturation. If at high stimulus levels each monaural input strongly activates an EE-cell, i.e., near to its maximal firing rate, the binaural input cannot double the firing rate of the unit. As a consequence, the binaural activation will be smaller than the summed monaural activation resulting in an 'artificial' BD of the correct sign. However, the following considerations let significant contributions of saturated EE-cells to the BD appear unlikely. First, in a recent fMRI study by Krumbholz et al. (2005), the activation of various brain structures, among them the IC, was compared for monaural and binaural stimulation with broadband noise bursts. Activation to binaural stimulation was less than half of the summed monaural activation. The authors outline that this finding strongly argues against a saturation mechanism which would yield a binaural response at least as large as the monaural response for EE-interaction and conclude that a suppressive mechanism, e.g., inhibition must be responsible for the strong reduction. Second, EE-cells are facilitated, i.e., fire stronger to binaural than to (summed) monaural stimulation only at ITDs near the best ITD of the cell. Near the worst ITD, EE-cells fire below each of the monaural rates, often they cease to fire at all (Yin and Chan, 1990). Since the inhibitory ITD-range of EE-cells seems to be at least as broad as the excitatory range, one would expect a larger overall contribution of IE-interaction compared to EE-interaction from MSO cells. Third, click stimuli are traditionally used in BD studies. Since clicks have most of their energy in the high frequency region and this region is activated more synchronously than the low frequency region due to the larger traveling wave velocity, it is not surprising that the ABR, and subsequently also the BD, is dominated by high-frequency contributions. Goksoy et al. (2005) measured that more than 80% of the spectral power of a click of 0.1 ms duration is located at frequencies larger than 1 kHz. Although the chirp stimulus used in the present study better synchronizes the lower frequencies, the weighting between low and high frequencies is similar to the click because the spectrum of the chirp used was flat and comparable to to click spectrum. Finally, Gaumond and Psaltikidou (1991) compared an EE- and an IE-model of binaural interaction and showed that only the latter can describe the linear relationship between BD amplitude and stimulus level. A constant ratio $BD/B = 0.2$ independent from stimulus level was reported by Riedel and Kollmeier (2002b).

The fact that the cat BD model of Ungan et al. (1997) using IE-interaction was successfully applied to guinea pig by Goksoy et al. (2005) and to man in the present study, further supports the hypothesis that the LSO plays a dominant role in BD generation. In a seminal paper, Ungan and Yagcioglu (2002) simultaneously measured BDs from a vertex electrode and a deep electrode in the LSO and the lateral lemniscus (LL) in cat. DN1 amplitude and latency as function of the ITD corresponded with the field potential measured at the level of the LL. They concluded that the BD component DN1 measured at the vertex is mainly due to

the contralateral inhibition of the lemniscal field potentials that result from the discharge activity of IE-cells in the LSO. Additionally, at the level of the SOC, Ungan and Yagcioglu (2002) demonstrated a bilateral asymmetry of the BD showing a stronger response to contralateral leading stimuli. This study strongly supports the hypothesis that the IE-cells in the LSO are the main BD generators and validates the IE-model of binaural interaction. Although the Jeffress model postulating EE-interaction has been the prevailing model for many decades, the first model using IE-interaction was suggested by von Bèkèsy (1930) and was later modified by van Bergeijk (1962) and Hall (1965) using the data of an early SO study by Galambos et al. (1959). The main difference between the two model types is that the Jeffress model forms a place map of azimuth using delay lines, while the IE-model uses the population activity, i.e., the relative activity of left and right LSO, but no delay lines to code for azimuth. Breebaart et al. (2001) successfully used a binaural model using IE-units and delay lines to explain psychoacoustical data. The existence of delay lines has been demonstrated in the avian system (e.g., Young and Rubel, 1983; Carr and Konishi, 1988, 1990; Overholt et al., 1992; Konishi, 2003). However, it is challenged in recent studies in mammals (McAlpine et al., 2001; Brand et al., 2002; McAlpine and Grothe, 2003; Campbell and King, 2004) and corresponding modeling work (Harper and McAlpine, 2004; Hancock and Delgutte, 2004).

Besides being important in research aiming to understand binaural interaction in the human brain stem, binaural difference potentials may also have clinical applications. Gopal and Kowalski (1999) showed a significant reduction of the BD amplitude in a group of children suffering from central auditory processing disorders (CAPDs) compared to a control group. Using the presence of the BD, Delb (2003) obtained a sensitivity and specificity of 76% to distinguish CAPD patients from normal subjects and concluded that BDs might have some diagnostic value in CAPD patients. In a recent paper, Wagner et al. (2005) investigated the clinical use of acoustically and electrically evoked BDs and found a good correlation between the presence of a BD and the ability of the subjects to utilize ITDs for azimuthal localization. They emphasize that at least three to five different values of the ITD are necessary to use BDs for prognostic purposes.

In summary, the IE-model not only correctly describes the dependence of BD amplitude and latency on the ITD, but also provides simulated BD waveforms. The significant BD amplitudes for large ITDs outside the physiological range and the nonlinear latency increase of the BD are not in accordance with the Jeffress model. Although the employed model well explains the BD data with only four parameters, it would presumably be insightful to design a more sophisticated model incorporating cochlear processing and neural transduction, e.g., on based on the work by Dau (2003). Such a model could reveal if the relatively large BD at long unphysiological ITDs as well as the monotonic decline of BD amplitude with increasing ITD simply are a consequence of the 'ringing' of the cochlear filters or not. If so, classical interpretations of the BD against the background of the Jeffress model would have to be regarded as rather artificial.

The measurement of binaural difference potentials is quite cumbersome due to their small amplitude and low SNR. Additionally, the interpretation of BDs is complicated because they are derived potentials and because contributions of IE- and EE-interactions cannot be unequivocally disentangled. Therefore, alternative methods that could directly measure binaural processing in the human brain stem would be highly desirable. Delb et al. (2004) suggested a time-scale feature extraction scheme to reveal binaural interaction from the measurement to binaural stimulation alone, i.e., without measuring and subtracting monaural responses. The features are so-called 'morphological local discriminant bases coefficients'. The analysis showed that the first coefficient is larger for binaural than for summed monaural stimulation, however, there was considerable overlap that grew with increasing ITD. It would be far more convincing if specific binaural potentials, i.e., evoked potentials that do not evoke any monaural response could be measured. Such potentials have been described in the long-latency domain for changes of interaural parameters of broadband noise (Halliday and Callaway, 1978; McEvoy et al., 1990; Jones et al., 1991; Jones, 1991; McEvoy et al., 1991a,b; Picton et al., 1991) and click trains (Ungan et al., 1989; Sams et al., 1993; McEvoy et al., 1993; Ungan and Ozmen, 1996; Ungan et al., 2001). Nevertheless, to the best knowledge of the authors, the assertions by McEvoy et al. (1990) and Jones et al. (1991) that no specific binaural potential of short latency has yet been demonstrated, still hold. Therefore, despite their disadvantages, BDs remain the only evoked potential method known to noninvasively analyze binaural processing in the human brain stem.

Acknowledgements

At first, the authors sincerely thank Prof. Pekcan Ungan for making available the matlab code of his cat BD model to us. In addition, we would like to thank the reviewers for their helpful comments. The present work was supported by the *Deutsche Forschungsgemeinschaft* through the *Sonderforschungsbereich Neurokognition* (SFB 517).

Appendix A

It is proven here that the SNR of the BD in a multi-ITD-experiment with two monaural and b binaural stimuli is optimized by choosing the monaural and binaural sweep numbers, N_M and N_B, respectively, according to

$$\frac{N_{M,opt}}{N_{B,opt}} = \sqrt{b} \tag{A.1}$$

instead of using the same sweep number for the three measurements. Thereby the total number of sweeps

$N =: N_B + N_L + N_R$ is not changed, i.e., the measurement time is not prolonged. The amount of the increase of the SNR or, vice versa, the decrease of the measurement time under conservation of the SNR is also deduced.

The same suppositions needed to prove the $1/N$-law for the decrease of the variance obtained by averaging over N sweeps have to be fulfilled. All sweeps contain a fixed signal s and additive zero-mean Gaussian noise with variance σ_0^2. The sweeps are neither correlated with the signal nor with all the other sweeps. With these assumptions it can be derived that

$$\sigma^2 = \frac{\sigma_0^2}{N}. \tag{A.2}$$

For the calculation of the variance of the binaural difference potential BD the variances of the three measurements are added assuming their mutual independence. Given that B, L and R were averaged from N_B, N_L and N_R sweeps, respectively, and that the sweeps of all three measurements have the same variance σ_0^2, the variance of the BD is

$$\sigma_{BD}^2 = \frac{\sigma_0^2}{N_B} + \frac{\sigma_0^2}{N_L} + \frac{\sigma_0^2}{N_R}. \tag{A.3}$$

In the case that equal sweep numbers entered the three averages ($N_B = N_L = N_R$), Eq. (A.3) reduces to

$$\sigma_{BD,eq}^2 = 3\frac{\sigma_0^2}{N_B} = 9\frac{\sigma_0^2}{N}. \tag{A.4}$$

In a multi-ITD-experiment with b binaural stimulus conditions, the two monaural responses are used b times to calculate b BDs. It is therefore better to measure the monaural potentials more accurately, i.e., with a higher sweep number $N_M =: N_L = N_R$. The sweep number of the binaural conditions is reduced accordingly to preserve the total number of sweeps N:

$$N = bN_B + 2N_M \Longleftrightarrow N_M = \frac{1}{2}(N - bN_B) \tag{A.5}$$

The variance of the BD can now be written as

$$\sigma_{BD}^2 = \frac{\sigma_0^2}{N_B} + 2\frac{\sigma_0^2}{N_M} = \sigma_0^2\left(\frac{1}{N_B} + \frac{4}{N - bN_B}\right). \tag{A.6}$$

An extremum of σ_{BD}^2 is found where the first derivative with respect to N_B vanishes:

$$0 = \frac{\partial\sigma_{BD}^2}{\partial N_B} = \sigma_0^2\left(-\frac{1}{N_B^2} + \frac{4b}{(N - bN_B)^2}\right). \tag{A.7}$$

The resulting quadratic equation uniquely reveals the optimal number of binaural sweeps as

$$N_{B,opt} = \frac{N}{b + 2\sqrt{b}}. \tag{A.8}$$

With Eq. (A.5) it is easily derived that the optimal sweep number for the monaural stimuli is

$$N_{M,opt} = \frac{N\sqrt{b}}{b + 2\sqrt{b}}. \tag{A.9}$$

The quotient of Eqs. (A.9) and (A.8) is $\sqrt{b}$ which is the proof of Eq. (A.1). Generalization of Eq. (A.4) for $b \geqslant 1$ yields the variance for case of equal sweep numbers of the monaural and binaural stimuli:

$$\sigma_{BD,eq}^2 = 3(b+2)\frac{\sigma_0^2}{N}. \tag{A.10}$$

On the other hand the variance of the BD for the optimized sweep numbers is

$$\sigma_{BD,opt}^2 = \frac{\sigma_0^2}{N_{B,opt}} + 2\frac{\sigma_0^2}{N_{M,opt}} = (\sqrt{b}+2)^2\frac{\sigma_0^2}{N}. \tag{A.11}$$

The advantage of the optimized stimulus paradigm can be expressed in terms of the quotient of the variances of the BDs:

$$q^2 =: \frac{\sigma_{BD,opt}^2}{\sigma_{BD,eq}^2} = \frac{b + 4\sqrt{b} + 4}{3b + 6} < 1. \tag{A.12}$$

q is the reduction of residual noise of the BD achieved by the optimized paradigm, $1/q$ is the increase in SNR. If the SNR shall be maintained, the total number of sweeps can be reduced to q^2N.

References

Batra, R., Kuwada, S., Fitzpatrick, D.C., 1997a. Sensitivity to interaural temporal disparities of low- and high-frequency neurons in the superior olivary complex. I. Heterogeneity of responses. J. Neurophysiol. 78 (3), 1222–1236.

Batra, R., Kuwada, S., Fitzpatrick, D.C., 1997b. Sensitivity to interaural temporal disparities of low- and high-frequency neurons in the superior olivary complex. II. Coincidence detection. J. Neurophysiol. 78 (3), 1237–1247.

Boudreau, J.C., Tsuchitani, C., 1968. Binaural interaction in the cat superior olive s segment. J. Neurophysiol. 31 (3), 442–454.

Brand, A., Behrend, O., Marquardt, T., McAlpine, D., Grothe, B., 2002. Precise inhibition is essential for microsecond interaural time difference coding. Nature 417 (6888), 543–547.

Brantberg, K., Hansson, H., Fransson, P., Rosenhall, U., 1999. The binaural interaction component in human ABR is stable within the 0- to 1-ms range of interaural time differences. Audiol. Neurootol. 4 (2), 88–94.

Breebaart, J., van de Par, S., Kohlrausch, A., 2001. Binaural processing model based on contralateral inhibition. I. Model structure. J. Acoust. Soc. Am. 110 (2), 1074–1088.

Caird, D., Klinke, R., 1983. Processing of binaural stimuli by cat superior olivary complex neurons. Exp. Brain Res. 52 (3), 385–399.

Campbell, R.A., King, A.J., 2004. Auditory neuroscience: a time for coincidence? Curr. Biol. 14 (20), R886–R888.

Carr, C.E., Konishi, M., 1988. Axonal delay lines for time measurement in the owl's brainstem. Proc. Natl. Acad. Sci. USA 85 (21), 8311–8315.

Carr, C.E., Konishi, M., 1990. A circuit for detection of interaural time differences in the brain stem of the barn owl. J. Neurosci. 10 (10), 3227–3246.

Dau, T., 2003. The importance of cochlear processing for the formation of auditory brainstem and frequency following responses. J. Acoust. Soc. Am. 113 (2), 936–950.

Dau, T., Wegner, O., Mellert, V., Kollmeier, B., 2000. Auditory brainstem responses with optimized chirp signals compensating basilar-membrane dispersion. J. Acoust. Soc. Am. 107 (3), 1530–1540.

Delb, W., 2003. Objektive Diagnostik der zentralen auditiven Verarbeitungs- und Wahrnehmungsstörung (AVWS) [Objective diagnosis of

central auditory processing and perception disorder]. HNO 51 (2), 99–103.

Delb, W., Strauss, D.J., Plinkert, P.K., 2004. A time-frequency feature extraction scheme for the automated detection of binaural interaction in auditory brainstem responses. Int. J. Audiol. 43 (2), 69–78.

Dobie, R.A., Berlin, C.I., 1979. Binaural interaction in brainstem-evoked responses. Arch. Otolaryngol. 105 (7), 391–398.

Dobie, R.A., Norton, S.J., 1980. Binaural interaction in human auditory evoked potentials. Electroencephalogr. Clin. Neurophysiol. 49 (3-4), 303–313.

Fitzpatrick, D.C., Kuwada, S., Batra, R., 2002. Transformations in processing interaural time differences between the superior olivary complex and inferior colliculus: beyond the Jeffress model. Hear. Res. 168 (1–2), 79–89.

Furst, M., Bresloff, I., Levine, R.A., Merlob, P.L., Attias, J.J., 2004. Interaural time coincidence detectors are present at birth: evidence from binaural interaction. Hear. Res. 187 (1–2), 63–72.

Furst, M., Eyal, S., Korczyn, A.D., 1990. Prediction of binaural click lateralization by brainstem auditory evoked potentials. Hear. Res. 49 (1–3), 347–359.

Furst, M., Levine, R.A., McGaffigan, P.M., 1985. Click lateralization is related to the beta component of the dichotic brainstem auditory evoked potentials of human subjects. J. Acoust. Soc. Am. 78 (5), 1644–1651.

Galambos, R., Schwartzkopff, J., Rupert, A., 1959. Microelectrode study of superior olivary nuclei. Am. J. Physiol. 197, 527–536.

Gaumond, R.P., Psaltikidou, M., 1991. Models for the generation of the binaural difference response. J. Acoust. Soc. Am. 89 (1), 454–456.

Gerull, G., Mrowinski, D., 1984. Brain stem potentials evoked by binaural click stimuli with differences in interaural time and intensity. Audiology 23 (3), 265–276.

Goksoy, C., Demirtas, S., Yagcioglu, S., Ungan, P., 2005. Interaural delay-dependent changes in the binaural interaction component of the guinea pig brainstem responses. Brain Res. 1054, 183–191.

Goldberg, J.M., Brown, P.B., 1968. Functional organization of the dog superior olivary complex: an anatomical and electrophysiological study. J. Neurophysiol. 31 (4), 639–656.

Goldberg, J.M., Brown, P.B., 1969. Response of binaural neurons of dog superior olivary complex to dichotic tonal stimuli: some physiological mechanisms of sound localization. J. Neurophysiol. 32 (4), 613–636.

Gopal, K.V., Kowalski, J., 1999. Slope analysis of auditory brainstem responses in children at risk of central auditory processing disorders. Scand. Audiol. 28 (2), 85–90.

Granzow, M., Riedel, H., Kollmeier, B., 2001. Single-sweep-based methods to improve the quality of auditory brain stem responses part I: Optimized linear filtering. Z. Audiol. 40 (1), 32–44.

Hall, J., 1965. Binaural interaction in the accessory superior-olivary nucleus of the cat. J. Acoust. Soc. Am. 37 (5), 814–823.

Halliday, R., Callaway, E., 1978. Time shift evoked potentials (TSEPs): method and basic results. Electroencephalogr. Clin. Neurophysiol. 45 (1), 118–121.

Hancock, K.E., Delgutte, B., 2004. A physiologically based model of interaural time difference discrimination. J. Neurosci. 24 (32), 7110–7117.

Harper, N.S., McAlpine, D., 2004. Optimal neural population coding of an auditory spatial cue. Nature 430 (7000), 682–686.

Hoth, S., 1986. Reliability of latency and amplitude values of auditory-evoked potentials. Audiology 25, 248–257.

Ito, S., Hoke, M., Pantev, C., Lütkenhöner, B., 1988. Binaural interaction in brainstem auditory evoked potentials elicited by frequency-specific stimuli. Hear. Res. 35 (1), 9–19.

Jasper, H.H., 1957. The ten twenty electrode system of the international federation. Electroenceph. Clin. Neurophys. 10, 371–375 (appendix).

Jeffress, L.A., 1948. A place theory of sound localization. J. Comp. Physiol. Psychol. 41, 35–39.

Jewett, D.L., Romano, M.N., Williston, J.S., 1970. Human auditory evoked potentials: possible brain stem components detected on the scalp. Science 167, 1517–1518.

Jiang, Z.D., 1996. Binaural interaction and the effects of stimulus intensity and repetition rate in human auditory brain-stem. Electroencephalogr. Clin. Neurophysiol. 100 (6), 505–516.

Jones, S.J., 1991. Memory-dependent auditory evoked potentials to change in the binaural interaction of noise signals. Electroencephalogr. Clin. Neurophysiol. 80 (5), 399–405.

Jones, S.J., Pitman, J.R., Halliday, A.M., 1991. Scalp potentials following sudden coherence and discoherence of binaural noise and change in the inter-aural time difference: a specific binaural evoked potential or a ''mismatch'' response? Electroencephalogr. Clin. Neurophysiol. 80 (2), 146–154.

Jones, S.J., Van der Poel, J.C., 1990. Binaural interaction in the brain-stem auditory evoked potential: evidence for a delay line coincidence detection mechanism. Electroencephalogr. Clin. Neurophysiol. 77 (3), 214–224.

Joris, P.X., 1996. Envelope coding in the lateral superior olive. II. Characteristic delays and comparison with responses in the medial superior olive. J. Neurophysiol. 76 (4), 2137–2156.

Joris, P.X., Smith, P.H., Yin, T.C., 1998. Coincidence detection in the auditory system: 50 years after Jeffress. Neuron 21 (6), 1235–1238.

Joris, P.X., Van de Sande, B., van der Heijden, M., 2004. Temporal damping in response to broadband noise. I. Inferior colliculus. J. Neurophysiol.

Joris, P.X., Yin, T.C., 1995. Envelope coding in the lateral superior olive. I. Sensitivity to interaural time differences. J. Neurophysiol. 73 (3), 1043–1062.

Joris, P.X., Yin, T.C., 1998. Envelope coding in the lateral superior olive. III. Comparison with afferent pathways. J. Neurophysiol. 79 (1), 253–269.

Kelly-Ballweber, D., Dobie, R.A., 1984. Binaural interaction measured behaviorally and electrophysiologically in young and old adults. Audiology 23 (2), 181–194.

Konishi, M., 2003. Coding of auditory space. Ann. Rev. Neurosci. 26, 31–55.

Krumbholz, K., Schönwiesner, M., Rübsamen, R., Zilles, K., Fink, G.R., von Cramon, D.Y., 2005. Hierarchical processing of sound location and motion in the human brainstem and planum temporale. Eur. J. Neurosci. 21 (1), 230–238.

Kuwada, S., Stanford, T.R., Batra, R., 1987. Interaural phase-sensitive units in the inferior colliculus of the unanesthetized rabbit: effects of changing frequency. J. Neurophysiol. 57 (5), 1338–1360.

Levine, R.A., 1981. Binaural interaction in brainstem potentials of human subjects. Ann. Neurol. 9 (4), 384–393.

Levine, R.A., Davis, P.J., 1991. Origin of the click-evoked binaural interaction potential, beta, of humans. Hear. Res. 57 (1), 121–128.

McAlpine, D., Grothe, B., 2003. Sound localization and delay lines – do mammals fit the model? Trends Neurosci. 26 (7), 347–350.

McAlpine, D., Jiang, D., Palmer, A.R., 1996. Interaural delay sensitivity and the classification of low best-frequency binaural responses in the inferior colliculus of the guinea pig. Hear. Res. 97 (1–2), 136–152.

McAlpine, D., Jiang, D., Palmer, A.R., 2001. A neural code for low-frequency sound localization in mammals. Nat. Neurosci. 4 (4), 396–401.

McEvoy, L., Hari, R., Imada, T., Sams, M., 1993. Human auditory cortical mechanisms of sound lateralization: II. Interaural time differences at sound onset. Hear. Res. 67 (1–2), 98–109.

McEvoy, L.K., Picton, T.W., Champagne, S.C., 1991a. Effects of stimulus parameters on human evoked potentials to shifts in the lateralization of a noise. Audiology 30 (5), 286–302.

McEvoy, L.K., Picton, T.W., Champagne, S.C., 1991b. The timing of the processes underlying lateralization: psychophysical and evoked potential measures. Ear. Hear. 12 (6), 389–398.

McEvoy, L.K., Picton, T.W., Champagne, S.C., Kellett, A.J., Kelly, J.B., 1990. Human evoked potentials to shifts in the lateralization of a noise. Audiology 29 (3), 163–180.

McPherson, D.L., Starr, A., 1993. Binaural interaction in auditory evoked potentials: brainstem, middle- and long-latency components. Hear. Res. 66 (1), 91–98.

McPherson, D.L., Starr, A., 1995. Auditory time-intensity cues in the binaural interaction component of the auditory evoked potentials. Hear. Res. 89 (1–2), 162–171.

Melcher, J.R., 1996. Cellular generators of the binaural difference potential in cat. Hear. Res. 95 (1–2), 144–160.

Nelder, J.A., Mead, R., 1965. A simplex method for function minimization. The Comput. J. 8, 308–313.

Overholt, E.M., Rubel, E.W., Hyson, R.L., 1992. A circuit for coding interaural time differences in the chick brainstem. J. Neurosci. 12 (5), 1698–1708.

Picton, T.W., Hillyard, S.A., Krausz, H.I., Galambos, R., 1974. Human auditory evoked potentials. I. Evaluation of components. Electroencephalogr. Clin. Neurophysiol. 36 (2), 179–190.

Picton, T.W., McEvoy, L.K., Champagne, S.C., 1991. Human evoked potentials and the lateralization of a sound. Acta Otolaryngol. Suppl. 491, 139–143, discussion 144.

Polyakov, A., Pratt, H., 1996. Evidence for spatio-topic organization of binaural processing in the human brainstem. Hear. Res. 94 (1–2), 107–115.

Pratt, H., Polyakov, A., Kontorovich, L., 1997. Evidence for separate processing in the human brainstem of interaural intensity and temporal disparities for sound lateralization. Hear. Res. 108 (1–2), 1–8.

Rayleigh, L.S.J.W., 1907. On our perception of sound direction. Philos. Mag. 13, 214–232.

Riedel, H., Granzow, M., Kollmeier, B., 2001. Single-sweep-based methods to improve the quality of auditory brain stem responses. part II: Averaging methods. Z. Audiol. 40 (2), 62–85.

Riedel, H., Kollmeier, B., 2002a. Auditory brain stem responses evoked by lateralized clicks: is lateralization extracted in the human brain stem? Hear. Res. 163 (1–2), 12–26.

Riedel, H., Kollmeier, B., 2002b. Comparison of binaural auditory brainstem responses and the binaural difference potential evoked by chirps and clicks. Hear. Res. 169 (1–2), 85–96.

Riedel, H., Kollmeier, B., 2003. Dipole source analysis of auditory brain stem responses evoked by lateralized clicks. Z. Med. Phys. 13 (2), 75–83.

Sams, M., Hämäläinen, M., Hari, R., McEvoy, L., 1993. Human auditory cortical mechanisms of sound lateralization: I. Interaural time differences within sound. Hear. Res. 67 (1–2), 89–97.

Sharbrough, F., Chatrian, G.-E., Lesser, R.P., Lüders, H., Nuwer, M., Picton, T.W., 1991. American electroencephalographic society guidelines for standard electrode position nomenclature. J. Clin. Neurophysiol. 8 (2), 200–202.

Sontheimer, D., Caird, D., Klinke, R., 1985. Intra- and extracranially recorded auditory evoked potentials in the cat. II. Effects of interaural time and intensity differences. Electroencephalogr. Clin. Neurophysiol. 61 (6), 539–547.

Stevens, S.S., Newman, E.B., 1936. The localization of actual sources of sound. Am. J. Psychol. 48, 297–306.

Stollman, M.H., Snik, A.F., Hombergen, G.C., Nieuwenhuys, R., ten Koppel, P., 1996. Detection of the binaural interaction component in the auditory brainstem response. Br. J. Audiol. 30 (3), 227–232.

Tsuchitani, C., 1988a. The inhibition of cat lateral superior olive unit excitatory responses to binaural tone bursts. I. The transient chopper response. J. Neurophysiol. 59 (1), 164–183.

Tsuchitani, C., 1988. The inhibition of cat lateral superior olive unit excitatory responses to binaural tone bursts. II. The sustained discharges. J. Neurophysiol. 59 (1), 184–211.

Ungan, P., Ozmen, B., 1996. Human long-latency responses to brief interaural disparities of intensity. Electroencephalogr. Clin. Neurophysiol. 99 (5), 479–490.

Ungan, P., Sahinoglu, B., Utkucal, R., 1989. Human laterality reversal auditory evoked potentials: stimulation by reversing the interaural delay of dichotically presented continuous click trains. Electroencephalogr. Clin. Neurophysiol. 73 (4), 306–321.

Ungan, P., Yagcioglu, S., 2002. Origin of the binaural interaction component in wave p4 of the short-latency auditory evoked potentials in the cat: evaluation of serial depth recordings from the brainstem. Hear. Res. 167 (1–2), 81–101.

Ungan, P., Yagcioglu, S., Goksoy, C., 2001. Differences between the N1 waves of the responses to interaural time and intensity disparities: scalp topography and dipole sources. Clin. Neurophysiol. 112 (3), 485–498.

Ungan, P., Yagcioglu, S., Özmen, B., 1997. Interaural delay-dependent changes in the binaural difference potential in cat auditory brainstem response: implications about the origin of the binaural interaction component. Hear. Res. 106 (1–2), 66–82.

van Bergeijk, W.A., 1962. Variation on a theme of bèkèsy: a model of binaural interaction. J. Acoust. Soc. Am. 34 (8, Pt. 2), 1431–1437.

von Bèkèsy, G., 1930. Zur Theorie des Hörens. Über das Richtungshören bei einer Zeitdifferenz oder Lautstärkenungleichheit der beiderseitigen Schalleinwirkungen. Physik. Z. 31, 857–868, 824–35.

Wada, S., Starr, A., 1989. Anatomical bases of binaural interaction in auditory brain-stem responses from guinea pig. Electroencephalogr. Clin. Neurophysiol. 72 (6), 535–544.

Wagner, H., Gräbel, S., Shehata-Dieler, W., Müller, J., 2005. Klinische Nutzung der binauralen Interaktionskomponente in akustisch bzw. elektrisch evozierten auditorischen Hirnstammpotentialen (A-BAEP bzw. E-BAEP) [Clinical use of the binaural interaction component in acoustically and/or electrically evoked auditory brainstem potentials (A-BAEP and/or E-BAEP)]. Z. Audiol. 44 (4), 174–185.

Walger, M., Stotzer, S., Meister, H., Foerst, A., von Wedel, H., 2003. Elektrophysiologische und psychoakustische Untersuchungen zur binauralen Signalverarbeitung normalhörender Erwachsener [Examination of binaural signal processing in normally hearing subjects using electrophysiological and psychoacoustical measurements]. HNO 51 (2), 125–133.

Wightman, F.L., Kistler, D.J., 1992. The dominant role of low-frequency interaural time differences in sound localization. J. Acoust. Soc. Am. 91 (3), 1648–1661.

Wrege, K.S., Starr, A., 1981. Binaural interaction in human auditory brainstem evoked potentials. Arch. Neurol. 38 (9), 572–580.

Yin, T.C., Chan, J.C., 1990. Interaural time sensitivity in medial superior olive of cat. J. Neurophysiol. 64 (2), 465–488.

Yin, T.C., Chan, J.C., Carney, L.H., 1987. Effects of interaural time delays of noise stimuli on low-frequency cells in the cat's inferior colliculus. III. Evidence for cross-correlation. J. Neurophysiol. 58 (3), 562–583.

Young, S.R., Rubel, E.W., 1983. Frequency-specific projections of individual neurons in chick brainstem auditory nuclei. J. Neurosci. 3 (7), 1373–1378.